Tuning Size and Size Distribution of Colloidal InAs Nanocrystals via Continuous Supply of Prenucleation Clusters on Nanocrystal Seeds

Sudarsan Tamang,[†,‡] Sunghee Lee,[†] Hyekyoung Choi,[†,§] and Sohee Jeong[*,†,§]

[†]Department of Nanomechatronics, Korea Institute of Machinery and Materials, Daejeon 34103, Korea
[‡]Department of Chemistry, Sikkim University, Gangtok, Sikkim 737102, India
[§]Department of Nanomechatronics, Korea University of Science and Technology (UST), Daejeon 34113, Korea

Ⓢ *Supporting Information*

Colloidal quantum dots (QDs) exhibit unique size-dependent optical and electrical properties due to quantum confinement. However, the true benefit of such unique quantum size effects depends on the ability to synthesize QDs of a wide range of sizes with a narrow size distribution at high reaction yield. One way to control size is by the separation of nucleation and growth.[1] A short "burst" of nucleation results in a sudden drop of monomer concentration below the critical level, thus terminating further nucleation.[2−4] Slow growth of the nanocrystals then follows, with no separate nucleus being formed, resulting in monodispersity.

More commonly, precursor reactivity is carefully tuned to control reaction yield, size, and size distribution.[5−10] Although this approach has been extremely successful with II–VI and IV–VI QDs, recent studies clearly suggest that it has failed to achieve the same degree of size and size distribution control with III–V QDs including InAs.[11,12] Therefore, despite their superior electronic and optoelectronic properties in bulk form compared to Pb or Cd based semiconductors integration of colloidal III–V QDs into solid state devices is highly impeded due to synthetic challenges. For example, the synthesis of monodisperse InAs QDs (2.5−6 nm) typically involves exhaustive postsynthesis size selective precipitation.[13−15] Attempts to replace the reactive precursor with a more stable one, which expected to release slowly the monomers for an extended period of time, thereby increasing size and monodispersity, have been met with little success. For example, by replacing the Si atom in tris(trimethylsilyl)arsenide ((TMS)$_3$As), Harris et al.[16] showed slight improvement in the size dispersion of InAs QDs, but the size range could not be increased. Similar attempts for InP QDs by Joung et al.[17] and Gary et al.[11] noted the slight increase in the average size of the particles by tuning precursor reactivity, whereas the size dispersion could not be improved.

In fact, there is growing consensus on the benefits of exploring alternative "non-classical" theoretical models and experimental set-ups to solve the problems of III–V QDs.[4,12,18−20] Recent observation of stable prenucleation clusters (PNCs) in the initial early stages of the reaction has led several research groups to question the correctness of the classical single-nucleation event.[21−25] Many of these studies performed on various materials including CaCO$_3$[21,22] and Fe$_3$O$_4$[26] have demonstrated that the formation of crystals results from the accretion of the PNCs rather than the direct accretion of atoms. Therefore, two or more nucleation events have been proposed instead of the single nucleation suggested

by classical theory. In other words, the PNCs may directly serve as "monomers" for secondary nucleation events *via* the aggregation pathway. On the other hand, there are also suggestions of redissolution of these PNCs, resulting in the generation of classical monomers for nucleation and growth.[18] In this respect, there have been few attempts on the synthesis with the magic-sized clusters (MSCs) to produce high quality III–V QDs.[18,27,28] In these studies MSCs have been identified as important intermediates in nanocrystal growth, yet the decisive role of these intermediate clusters in size evolution has not been clearly demonstrated.

We report here the detection of ultrasmall amorphous InAs PNCs with 1.8 nm in diameter synthesized at room temperature when commonly employed InAs precursors, namely, indium oleate (In(oleate)$_3$) and (TMS)$_3$As, were reacted under a N$_2$ atmosphere. The reaction was exothermic, as noted from the slight temperature increase in the reaction mixture. ^{1}H nuclear magnetic resonance (NMR) confirms that (TMS)$_3$As reacted with In(oleate)$_3$ to form the TMS-oleate (Figure S1) at room temperature. The isolated nanoclusters are In-rich, with an In/As ratio of about 2.3 as measured by inductively coupled plasma-atomic emission spectroscopy (ICP-AES) (Table S1). These nanoclusters were not uniform in size, as evident in both absorption spectroscopy and transmission electron microscopy (TEM) results (Figure 1). According to the selected area electron diffraction (SAED) pattern (Figure S2), it can be inferred that our InAs PNCs exhibit an amorphous phase. In addition, powder X-ray
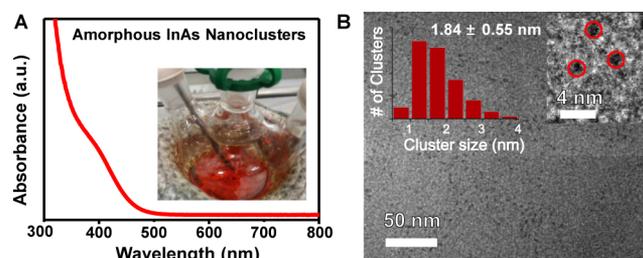
Figure 1. (A) Absorption spectra of ultrasmall amorphous InAs nanoclusters. (B) TEM image and size-distribution of the synthesized nanoclusters.

diffraction (XRD) analysis performed further on isolated powder showed that these clusters were amorphous in nature (Figure 3E). High-resolution TEM also confirmed the amorphous nature of the particles. These results indicate that our synthesized nanoclusters differ from typical InAs MSCs in that (1) the reported formation temperature is typically high, at over 150 °C, and (2) they have distinct absorption features at 420 and 460 nm.[27,28]

More notably, when the temperature of the cluster solution was carefully increased, we observed continuous growth behavior, which is again a feature that is unusual for typical MSCs (Figures S3 and S4). The MSCs are resistant to growth marked by the presence of persistent characteristic absorption features when the reaction temperature is changed. This control experiment allowed us to distinguish our ultrasmall amorphous PNCs (absorption ~400 nm) from InAs MSCs.[27,28]

According to the classical model, in absence of Ostwald ripening, the rate of diffusion controlled growth is inversely propositional to the size ($dr/dt \propto 1/r$), i.e., smaller particles will grow at faster rates than larger ones, and the size distribution narrows with time.[29−31] This phenomenon, referred to as focusing, is illustrated in Figure 2A. To achieve size-focused

Figure 3. (A) Size tunability with access to larger particles. Representative UV−vis−NIR spectra of differently sized InAs QDs synthesized by externally supplying the monomers via the controlled injection of amorphous nanocluster solution (at 0.005 mmol/min, temperature 270 °C). (B, C) Representative TEM images of 5.79 ± 0.43 nm (7.5%) InAs QDs (C) synthesized from 2.54 ± 0.42 nm (16.3%) seeds (B). (D) Relative size distribution represented by the HWHM of the first excitonic peak of InAs QDs synthesized by adding 0.05 to 3 mmol (filled circles) of precursor solutions compared with the initial seed solution (green). Empty circles represented literature values for high-quality PbS QDs for comparison.[28] (E) XRD spectra of InAs nanoclusters, InAs "seeds", and the InAs QDs.

Figure 2. (A) Illustration of the "size-focused" growth in which smaller nanocrystals (r_1) grow faster than larger ones (r_2), resulting in better size uniformity as the reaction progresses. Only two sized nanocrystals (blue dots) have been shown for simplicity. Red dots symbolize "monomers." (B) Synthetic scheme of growth of InAs QDs: slow and continuous injection of amorphous PNC solutions into preformed InAs QD "seeds" using a syringe pump.

growth of InAs QDs, we use the prepared PNCs as a direct source of monomers. The cluster solution was directly injected into preformed InAs nanocrystal "seeds" (Figure 2B). In classical terms, the seeded approach is an effective way to separate nucleation and growth.[30]

In our experiment, we first synthesized InAs QD "seeds" capped with oleic acid using a typical hot injection technique. The InAs QD "seeds" showed a typical broad first excitonic peak ($1S_e−1S_h$) around 1.77 eV, namely, 700 nm (Figure 3A, green), with half-width at half-maximum (HWHM) > 100 meV (Figure 3D). TEM images show that the size distribution is about 16.3% (Figure 3B). Typically, the chemical yield of this hot injection reaction is ~40%. To this polydispersed "seed" solution was injected amorphous InAs nanocluster solution in ODE at different rates using a syringe pump at specific growth temperatures. Figure 3A presents the ultraviolet−visible-near-infrared (UV−vis-NIR) spectra of differently sized InAs QDs

synthesized by slow and continuous injection (at 0.005 mmol/min) of InAs QD "seed" solution.

This slow and continuous injection resulted in further growth of the InAs QDs, as well as an increase in the size uniformity (Figure 3C), as reflected in sharpening of the absorption first excitonic peak ($1S_e−1S_h$). Figure 3D shows that the HWHM of the variously sized InAs QDs with our method was comparable to HWHM recently achieved with PbS QDs, having a similar first excitonic peak position (1.5−1.2 eV).[32] The size distribution of the InAs QDs decreases as a function of their sizes, confirmed by the TEM analysis (Figures S6 and S7).

This result is consistent with the prediction of classical diffusion-controlled growth of the QDs under high super-saturation of monomers. In other words, these amorphous nanoclusters are indeed a reliable source of monomers, irrespective of whether monomers are generated via dissolution of the clusters or direct accretion to growing crystal (in which case, the clusters are the monomers). In this synthetic scheme, since the final size of the product depends solely on the amount of solution of precursor externally added at a fixed growth temperature, the reaction can be stopped at any desired time. This method thus allows the preparation of InAs QDs with a wide size range and high degree of tunability and reproducibility. For example, by stopping the precursor supply and

removing the heat source at a desired interval, two samples with an excitonic peak difference of as little as 5−10 nm with size dispersity <10% can be isolated. Such precise control of size and size dispersion is otherwise extremely difficult in III-V QDs when the monomer reservoir is internally controlled by controlling precursor reactivity. When the monomer concentration approaches equilibrium solubility, smaller particles dissolve while larger ones keep growing, resulting in broad size distribution (Ostwald ripening).[30−33] Maintaining the monomer reservoir internally is difficult as the precursor depletion is a major concern in III-V QD synthesis.[34]

An alternative way of maintaining the monomer reservoir during the growth stage is by supplying the precursor externally as demonstrated by Peng et al., using molecular precursors.[35] We carefully monitored the growth of InAs QDs using absorption spectra when molecular precursors of In(oleate)$_3$ and (TMS)$_3$As were continuously supplied during the synthesis with various experimental conditions (Figure S5), in contrast to the injection of an equivalent concentration of our amorphous nanoclusters under the same reaction condition (Figure S8). In the case of the continuous molecular precursor injection, we observed initial size focusing and red-shift in the first excitonic absorption peak, similar to Peng's previous observation.[35] Interestingly, the particle size distribution again increased while rate of the increase in size decreased after initial focusing stage despite continuous injection of molecular precursors in all experimental conditions we explored as reflected in their HWHM and $1S_e$−$1S_h$, respectively. (Figure 4, black line)
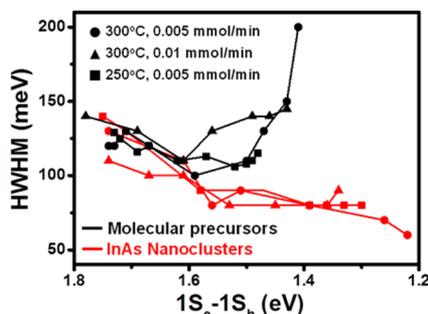
Figure 4. HWHM was plotted as a function of the first excitonic peak from Figure S8 to visualize their size distribution during the course of growth using molecular precursors (black line) and InAs nanoclusters (red line) in various experimental conditions: 300 °C of injection temperature with 0.005 mmol/min of feeding rate (circle), 300 °C of injection temperature with 0.01 mmol/min of feeding rate (triangle), and 250 °C of injection temperature with 0.01 mmol/min of feeding rate (square), respectively.

Accumulation of precursors can lead to formation of isolated QDs due to involvement of multiple competing precursor conversion steps. In contrast, our results indicate that by supplying the InAs nanocluster solution externally, the monomer reservoir can be effectively consumed in the growth stages, which results in focusing of nanocrystal sizes with the increasing particle diameter. The use of our amorphous PNCs efficiently circumvents the complex precursor conversion pathways, thus resulting in reliability and reproducibility in synthesis.

We also observed a dramatic increase in reaction yield from the typical level of ∼40% to up to 75%. Measuring the absorbance at high photon energy (450 nm)[36] allows us to determine precisely the size-independent concentration of QDs

and, hence, the reaction yields (Figure S9 and Table S2). The increase in the reaction yield indicates that the slow injection of an intermediate cluster eliminates the adverse effects of precursor depletion, which is another advantage of our InAs QDs synthesis. Both temperature and injection rate are decisive in determining the final size and size dispersion (Figures S10 and S11). An injection of 3 mmol precursor at 270 °C gave InAs QDs with $1S_{max}$ at 937 and 1110 nm as the rate decreased from 0.05 to 0.005 mmol/min. Similarly, larger particles could be synthesized by increasing the temperature.

In conclusion, we have identified amorphous InAs PNCs as an important intermediate in the nucleation and growth of InAs QDs. These clusters synthesized at room temperature were more stable than the molecular precursors (group V), but less stable than MSCs, making them suit as a single-source precursor for the synthesis of InAs QDs with narrow size distribution. As an alternative to search for newer precursors with optimum reactivity, we developed a simple approach to control the size and size distribution of InAs QDs using the existing precursors. Highly monodisperse InAs QDs (<10%) in the size range of ∼3 to 6 nm were synthesized by continuous supplying preformed amorphous InAs PNCs into InAs nanocrystal "seeds". Unprecedented control over the size of the InAs QDs can be achieved by simply adjusting the rate of injection, reaction temperature, and growth time. The observation of remarkably strong size-focusing growth, using amorphous PNCs instead of molecular precursors as the monomer source, demonstrates that irrespective of whether nanocrystal formation involves a single-step or multiple-step nucleation event, each step is governed, at least qualitatively, by classical nucleation and growth theory. The approach could be equally relevant for other III-V QDs with similar bonding and precursor chemistry, perhaps provided that the growth is under diffusion-controlled mode.

■ ASSOCIATED CONTENT

ⓢ Supporting Information

The Supporting Information is available free of charge on the ACS Publications website at DOI: 10.1021/acs.chemmater.6b03585.

Experimental details, molar extinction coefficient calculation, XRD patterns, TEM images, absorbance spectrum, ICP data, NMR spectrum, plot of HWHM as a function of first excitonic peaks (PDF)

■ AUTHOR INFORMATION

Corresponding Author
*S. Jeong. E-mail: sjeong@kimm.re.kr.

Notes
The authors declare no competing financial interest.

■ ACKNOWLEDGMENTS

■ REFERENCES

(1) LaMer, V. K.; Dinegar, R. H. Theory, Production and Mechanism of Formation of Monodispersed Hydrosols. *J. Am. Chem. Soc.* **1950**, 72, 4847−4854.

(2) Kwon, S. G.; Hyeon, T. Formation Mechanisms of Uniform Nanocrystals via Hot-Injection and Heat-Up Methods. *Small* **2011**, *7*, 2685−2702.

(3) Reiss, P.; Carriere, M.; Lincheneau, C.; Vaure, L.; TaMang, S. Synthesis of Semiconductor Nanocrystals, Focusing on Nontoxic and Earth-Abundant. *Chem. Rev.* **2016**, *116*, 10731.

(4) Tamang, S.; Lincheneau, C.; Hermans, Y.; Jeong, S.; Reiss, P. Chemistry of InP Nanocrystal Syntheses. *Chem. Mater.* **2016**, *28*, 2491−2506.

(5) Steckel, J. S.; Yen, B. K. H.; Oertel, D. C.; Bawendi, M. G. On the mechanism of Lead Chalcogenide Nanocrystal Formation. *J. Am. Chem. Soc.* **2006**, *128*, 13032−13033.

(6) Hendricks, M. P.; Campos, M. P.; Cleveland, G. T.; Plante, I. J. L.; Owen, J. S. A tunable library of substituted thiourea precursors to metal sulfide nanocrystals. *Science* **2015**, *348*, 1226−1230.

(7) Guzelian, A. A.; Banin, U.; Kadavanich, A. V.; Peng, X.; Alivisatos, A. P. Colloidal chemical synthesis and characterization of InAs nanocrystal quantum dots. *Appl. Phys. Lett.* **1996**, *69*, 1432−1434.

(8) Liu, H.; Owen, J. S.; Alivisatos, A. P. Mechanistic Study of Precursor Evolution in Colloidal Group II-VI Semiconductor Nanocrystal Synthesis. *J. Am. Chem. Soc.* **2007**, *129*, 305−312.

(9) Abe, S.; Capek, R. K.; Geyter, B. D.; Hens, Z. Tuning the Postfocused Size of Colloidal Nanocrystals by the Reaction Rate: From Theory to Application. *ACS Nano* **2012**, *6*, 42−53.

(10) Kim, K.; Yoo, D.; Choi, H.; Tamang, S.; Ko, J.-H.; Kim, S.; Kim, Y.-H.; Jeong, S. Halide-Amine Co-Passivated Indium Phosphide Colloidal Quantum Dots in Tetrahedral Shape. *Angew. Chem., Int. Ed.* **2016**, *55*, 3714−3718.

(11) Gary, D. C.; Glassy, B. A.; Cossairt, B. M. Investigation of Indium Phosphide Quantum Dot Nucleation and Growth Utilizing Triarylsilylphosphine Precursors. *Chem. Mater.* **2014**, *26*, 1734.

(12) Franke, D.; Harris, D. K.; Xie, L.; Jensen, K. F.; Bawendi, M. G. The Unexpected Influence of Precursor Conversion Rate for III−V Quantum Dots. *Angew. Chem.* **2015**, *127*, 14507−14511.

(13) Soreni-Harari, M.; Mocatta, D.; Zimin, M.; Gannot, Y.; Banin, U.; Tessler, N. Interface Modifications of InAs Quantum-Dots Solids and Their Effects on FET Performance. *Adv. Funct. Mater.* **2010**, *20*, 1005−1010.

(14) Guzelian, A.; Banin, U.; Kadavanich, A.; Peng, X.; Alivisatos, A. Colloidal Chemical Synthesis and Characterization of InAs Nanocrystal Quantum Dots. *Appl. Phys. Lett.* **1996**, *69*, 1432−1434.

(15) Yu, P.; Zhu, K.; Norman, A. G.; Ferrere, S.; Frank, A. J.; Nozik, A. J. Nanocrystalline TiO2 Solar Cells Sensitized with InAs Quantum Dots. *J. Phys. Chem. B* **2006**, *110*, 25451−25454.

(16) Harris, D. K.; Bawendi, M. G. Improved Precursor Chemistry for the Synthesis of III−V Quantum Dots. *J. Am. Chem. Soc.* **2012**, *134*, 20211−20213.

(17) Joung, S. M.; Yoon, S.; Han, C. S.; Kim, Y.; Jeong, S. Facile Synthesis of Uniform Large-sized InP Nanocrystal Quantum Dots using tris(tert-butyldimethylsilyl)phosphine. *Nanoscale Res. Lett.* **2012**, *7*, 93.

(18) Gary, D. C.; Terban, M. W.; Billinge, S. J. L.; Cossairt, B. M. Two-Step Nucleation and Growth of InP Quantum Dots via Magic-Sized Cluster Intermediates. *Chem. Mater.* **2015**, *27*, 1432−1441.

(19) Gary, D. C.; Flowers, S. E.; Kaminsky, W.; Petrone, A.; Li, X.; Cossairt, B. M. Single-Crystal and Electronic Structure of a 1.3 nm Indium Phosphide Nanocluster. *J. Am. Chem. Soc.* **2016**, *138*, 1510−1513.

(20) Lee, J.; Yang, J.; Kwon, S. G.; Hyeon, T. Nonclassical nucleation and growth of inorganic nanoparticles. *Nat. Rev. Mats.* **2016**, *1*, 16034.

(21) Gebauer, D.; Völkel, A.; Cölfen, H. Stable Prenucleation Calcium Carbonate Clusters. *Science* **2008**, *322*, 1819−1822.

(22) Pouget, E. M.; Bomans, P. H. H.; Goos, J. A. C. M.; Frederik, P. M.; With, G. D.; Sommerdijk, N. A. J. M. The Initial Stages of Template-Controlled CaCO₃ Formation Revealed by Cryo-TEM. *Science* **2009**, *323*, 1455−1458.

(23) Wallace, A. F.; Hedges, L. O.; Fernandez-Martinez, A.; Raiteri, P.; Gale, J. D.; Waychunas, G. A.; Whitelam, S.; Banfield, J. F.; Yoreo, J. J. D. Microscopic Evidence for Liquid-Liquid Separation in Supersaturated CaCO₃ Solutions. *Science* **2013**, *341*, 885−889.

(24) Dukes, A. D.; McBride, J. R.; Rosenthal, S. J. Synthesis of Magic-Sized CdSe and CdTe Nanocrystals with Diisooctylphosphinic Acid. *Chem. Mater.* **2010**, *22*, 6402−6408.

(25) Cossairt, B. M.; Owen, J. S. CdSe Clusters: At the Interface of Small Molecules and Quantum Dots. *Chem. Mater.* **2011**, *23*, 3114−3119.

(26) Baumgartner, J.; Dey, A.; Bomans, P. H.; Le Coadou, C.; Fratzl, P.; Sommerdijk, N. A.; Faivre, D. Nucleation and growth of magnetite from solution. *Nat. Mater.* **2013**, *12*, 310−314.

(27) Xie, R.; Peng, X. Synthetic Scheme for High-Quality InAs Nanocrystals Based on Self-Focusing and One-Pot Synthesis of InAs-Based Core−Shell Nanocrystals. *Angew. Chem., Int. Ed.* **2008**, *47*, 7677−7680.

(28) Xie, R.; Li, Z.; Peng, X. Nucleation Kinetics vs Chemical Kinetics in the Initial Formation of Semiconductor Nanocrystals. *J. Am. Chem. Soc.* **2009**, *131*, 15457−15466.

(29) Reiss, H. The Growth of Uniform Colloidal Dispersions. *J. Chem. Phys.* **1951**, *19*, 482−487.

(30) Sugimoto, T. Preparation of Monodispersed Colloidal Particles. *Adv. Colloid Interface Sci.* **1987**, *28*, 65−108.

(31) Clark, M. D.; Kumar, S. K.; Owen, J. S.; Chan, E. M. Focusing Nanocrystal Size Distributions via Production Control. *Nano Lett.* **2011**, *11*, 1976−1980.

(32) Choi, H.; Ko, J.-H.; Kim, Y.-H.; Jeong, S. Steric-Hindrance-Driven Shape Transition in PbS Quantum Dots: Understanding Size-Dependent Stability. *J. Am. Chem. Soc.* **2013**, *135*, 5278−5281.

(33) Kabalnov, A. S.; Shchukin, E. D. Ostwald Ripening Theory: Applications to Fluorocarbon Emulsion Stability. *Adv. Colloid Interface Sci.* **1992**, *38*, 69−97.

(34) Allen, P. M.; Walker, B. J.; Bawendi, M. G. Mechanistic Insights into the Formation of InP Quantum Dots. *Angew. Chem., Int. Ed.* **2010**, *49*, 760−762.

(35) Peng, X.; Wickham, J.; Alivisatos, A. P. Kinetics of II-VI and III-V Colloidal Semiconductor Nanocrystal Growth: "Focusing" of Size Distributions. *J. Am. Chem. Soc.* **1998**, *120*, 5343−5344.

(36) Yu, P.; Beard, M. C.; Ellingson, R. J.; Ferrere, S.; Curtis, C.; Drexler, J.; Luiszer, F.; Nozik, A. J. Absorption Cross-section and Related Optical Properties of Colloidal InAs Quantum Dots. *J. Phys. Chem. B* **2005**, *109*, 7084−7087.